Journal of Engineering Mathematics 21: 69–86 (1987)

A perturbation solution for compressible viscous channel flows

L.W. Schwartz
Corporate Research Laboratories, Exxon Research & Engineering Co., Annandale, NJ 08801, USA; present address: Department of Mechanical and Aerospace Engineering, Rutgers University, P.O. Box 909, Piscataway, NJ 08854, USA

Received 10 November 1986; accepted 24 November 1986

Abstract

The two-dimensional compressible Navier-Stokes equations are solved by a perturbation expansion in the parameter (Mach number)^2/Reynolds number. A fortieth-order solution is generated by a computer algorithm. These series are then summed as convergent series of diagonal Padé approximants. Effectively-exact solutions have been found for Reynolds numbers between zero and 1000 and a range of subsonic Mach numbers in the case of fully-developed isothermal flow between parallel side walls. Choking of the flow is shown to occur for a moderate value of channel Reynolds number. The two-dimensional velocity and pressure fields are obtained. The engineering assumption that friction factor is sensibly independent of Mach number may lead to significant underprediction of head loss in the laminar flow regime.

1. Introduction

In this paper we will discuss the effects of compressibility in two-dimensional channel flow of a viscous liquid. For simplicity, the discussion is restricted to isothermal laminar flows and effectively exact solutions of the compressible Navier-Stokes equations will be obtained.

Finite Mach number effects are important in a variety of applications. Although gas pipelines are usually run at low subsonic Mach numbers, there are significant changes in pressure due to the great lengths over which friction acts; thus the flow may not be treated as incompressible. On the other hand, the isothermal assumption is considered to be quite good for these flows, provided rapid variations in flow properties do not occur in which case an adiabatic assumption might well be more appropriate. The study of the laminar compressible regime is immediately applicable to high-speed gas flow through narrow passageways; i.e. the general field of gas-film lubrication. Typical applications include the design of externally-pressurized thrust bearings and pressure relief values. A number of other devices are discussed by Gross [5].

It is well known that multiphase mixtures have acoustic wave speeds that are remarkably low. Fox [4, p. 92], for example, gives data for mixtures of air and water. For almost the entire intermediate concentration range, the wave speed is roughly an order of magnitude less than the sound speed for either constituent alone. In these cases compressibility becomes important at quite moderate flow velocities.

The present study deals with the simplest of all realistic geometries: fully-developed flow between parallel side walls. The differential equations and boundary conditions are treated exactly, however. No simplifying assumptions, e.g. boundary layer or one-dimensional gasdynamic theories, are employed here. Certain other simple geometries, such as axisymmetric pipe flows, can be treated without major modification. Also, the perturbation technique to be presented here can, in principle, be applied to much more complicated flows.

The mathematical character of the solutions of the compressible Navier-Stokes equations has not been deeply explored. While a few closed-form solutions have been found, they are restricted to one-dimensional cases (see Pai [8, Chapter IV]). It is interesting to note that compressibility causes the system of equations to remain nonlinear even in the creeping-motion limit $\mathrm{Re} \to 0$. A number of solutions of the incompressible Navier-Stokes equations have been found and have been confirmed experimentally; their ability to predict fluid motion, within the appropriate parameter range, is beyond dispute. This statement cannot be made with equal enthusiasm in the compressible case. For example, Stokes' hypothesis that the bulk viscosity $\lambda + (2/3)\mu$ can be taken equal to zero has been used by virtually all subsequent authors. Indeed, we adopt it in the present work. It can be rigorously justified only for monatomic thermally-perfect gases and its general validity has been questioned by Lagerstrom [6, Section B.3] and others.

The present perturbation scheme is based on the principle of slow variation. That is, for sufficiently small viscosity and/or mass flow rate, flow properties can be expected to vary slowly with distance along the channel. To a first approximation, the velocity profile may be assumed to be parabolic, just as in the incompressible case. The magnitude of the velocity will increase, as the pressure and density decrease, down the channel, in such a way that mass flux is conserved. By appropriate nondimensionalization and rescaling of the governing equations, it becomes clear that the above, intuitive, solution is valid when the parameter $\hat{\epsilon} = \gamma \mathrm{M}^2/\mathrm{Re}$ is very small. Here M is the local average Mach number at a station and γ is the ratio of specific heats. In this report we develop the solution as a high-order perturbation series in $\hat{\epsilon}$. These series may then be summed very accurately through the use of Padé approximants.

The slow-variation principle is closely related to the thin- and slender-body theories. In the context of channel flow, Blasius [2] showed that incompressible flow in a channel of slowly varying cross-section could be computed as a series expansion in a parameter equivalent to the local wall slope. The leading term is the well-known Poiseuille solution. Blasius' series was extended to second order by Abramowitz [1]. Lucas [7], in an unpublished dissertation, developed a computer algorithm to extend the solution to very high order. He then used Padé summation and was able to compute, for example, laminar separation and reattachment in a divergent channel. A more general discussion of slow variations as a perturbation procedure in mechanics has recently been given by Van Dyke [11]. He points out that, in many cases, slow-variation approximations are much more powerful than the more common slight-variation approximations. Indeed, the former often have the desirable property that they are uniformly valid in space.

In Section 2 we state the full problem and develop an algorithm for generating coefficients in a series solution. By a similarity argument, based on the invariance of the solution to the choice of origin in the streamwise direction, it is shown that the number of independent variables can be reduced. Computed results are presented in Section 3. 'Mathematical choking' of the flow, i.e. the inability to analytically continue the solution past a station at which conditions are near-sonic, is demonstrated for $\mathrm{Re} \geqslant \mathrm{O}(10)$. Padé-summed pressure and velocity profiles are presented for a range of Reynolds and Mach numbers. We calculate the friction factor variation with Mach number and show that the usual definition of friction factor, based on one-dimensional theory, appears to be defective. This latter point is more fully discussed in Appendix I.

2. Formulation

We consider steady flow of a compressible fluid in a nominally infinite two-dimensional channel with parallel straight walls separated by a distance $2R$. Gravity and hence buoyancy effects will be neglected. Let $\tilde{x}$ and $\tilde{y}$ be cartesian coordinates in the streamwise and transverse

directions respectively. The flow field is assumed to be symmetric about the channel centerline $\tilde{y} = 0$. The fluid is taken to be a thermally perfect gas; thus the density and pressure are linearly related according to

$$\tilde{\rho} = \gamma \tilde{p}/a^2 \tag{1}$$

where γ is the ratio of specific heats and a, the sound speed, is a given constant by virtue of the isothermal assumption.

Denoting the velocity field by $(\tilde{u}, \tilde{v})$ and using equation (1), the continuity equation becomes

$$(\tilde{p}\tilde{u})_{\tilde{x}} + (\tilde{p}\tilde{v})_{\tilde{y}} = 0 \tag{2}$$

where subscripts signify partial differentiation. The constant mass-flow rate (per unit width) in each half-channel is given by

$$\dot{m} = \int_0^R \tilde{\rho}\tilde{u}\, \mathrm{d}\tilde{y}.$$

Equation (2) is satisfied identically by the streamfunction defined by

$$\tilde{\Psi}_{\tilde{y}} = \tilde{p}\tilde{u}, \quad \tilde{\Psi}_{\tilde{x}} = -\tilde{p}\tilde{v}. \tag{3a,b}$$

The $\tilde{x}$ and $\tilde{y}$ momentum equations may now be written as

$$\tilde{\Psi}_{\tilde{y}}\tilde{u}_{\tilde{x}} - \tilde{\Psi}_{\tilde{x}}\tilde{u}_{\tilde{y}} = -\frac{a^2}{\gamma}\tilde{p}_{\tilde{x}} + \frac{a^2}{\gamma}\mu\left(\tfrac{4}{3}\tilde{u}_{\tilde{x}\tilde{x}} + \tilde{u}_{\tilde{y}\tilde{y}} + \tfrac{1}{3}\tilde{v}_{\tilde{y}\tilde{x}}\right), \tag{4}$$

$$\tilde{\Psi}_{\tilde{y}}\tilde{v}_{\tilde{x}} - \tilde{\Psi}_{\tilde{x}}\tilde{v}_{\tilde{y}} = -\frac{a^2}{\gamma}\tilde{p}_{\tilde{y}} + \frac{a^2}{\gamma}\mu\left(\tfrac{4}{3}\tilde{v}_{\tilde{y}\tilde{y}} + \tilde{v}_{\tilde{x}\tilde{x}} + \tfrac{1}{3}\tilde{u}_{\tilde{y}\tilde{x}}\right), \tag{5}$$

where Stokes' hypothesis concerning the bulk viscosity, see Schlichting [9, pp. 57–60], has been invoked. Unlike the incompressible flow case where introduction of a streamfunction reduces the number of dependent variables without substantially complicating the governing equations, here the streamfunction is taken as an additional unknown in order to eliminate cubic products in the momentum equations. This results in a significant simplification in the mechanized perturbation calculations.

Equations (3) through (5), with suitable boundary conditions, determine the unknowns $\tilde{u}$, $\tilde{v}$, $\tilde{p}$, and $\tilde{\Psi}$. The no-slip boundary condition on the channel walls requires that

$$\tilde{u}(\tilde{x}, \pm R) = 0, \quad \tilde{v}(\tilde{x}, \pm R) = 0. \tag{6a,b}$$

The streamfunction is taken to vanish on $\tilde{y} = 0$, the channel centerline. On the walls it assumes the constant values

$$\tilde{\Psi}(\tilde{x}, \pm R) = \pm a^2\dot{m}/\gamma. \tag{6c}$$

The assumption of bilateral symmetry of the channel flow requires that $\tilde{u}$ and $\tilde{p}$ be even functions of $\tilde{y}$ while $\tilde{v}$ and $\tilde{\Psi}$ are odd functions. Selecting an arbitrary station along the channel as $\tilde{x} = 0$, we choose the wall pressure there as reference, i.e.

$$\tilde{p}(0, \pm R) = p_0. \tag{6d}$$

The problem may be made nondimensional by selecting R, p_0, and $a^2\dot{m}/\gamma$ as units of length, pressure, and streamfunction respectively. The reference velocity then becomes

$$u_{\text{ref}} = \frac{a^2\dot{m}}{\gamma p_0 R}.$$

u_{ref} is approximately equal to the mean value of the streamwise velocity at $\tilde{x} = 0$; it is not exactly the mean value however for, as will become apparent, compressible channel flows are characterized by a small transverse pressure, and hence density, variation. In terms of dimensionless (untilded) variables, the equations may be written as

$$\Psi_y = pu, \quad \Psi_x = -pv, \tag{7a,b}$$

$$\text{Re}\left(\Psi_y u_x - \Psi_x u_y\right) = -\frac{p_x}{\epsilon} + \tfrac{4}{3}u_{xx} + u_{yy} + \tfrac{1}{3}v_{yx}, \tag{8}$$

$$\text{Re}\left(\Psi_y v_x - \Psi_x v_y\right) = -\frac{p_y}{\epsilon} + \tfrac{4}{3}v_{yy} + v_{xx} + \tfrac{1}{3}u_{yx}. \tag{9}$$

The boundary conditions become

$$u(x, 1) = v(x, 1) = 0, \quad v(x, 0) = \Psi(x, 0) = 0, \quad \Psi(x, 1) = 1, \quad p(0, 1) = 1. \tag{10a,b,c,d}$$

The parameters in equations (8) and (9) are the Reynolds number based on the channel half-width

$$\text{Re} = \dot{m}/\mu \tag{11}$$

and

$$\epsilon = \left(a^2\mu\dot{m}\right)/\left(\gamma p_0^2 R^2\right) = \gamma \text{M}^2/\text{Re}. \tag{12}$$

Here $\text{M} = u_{\text{ref}}/a$, a characteristic Mach number at the station $x = 0$. Notice that the dimensional scaling of the problem has reduced the number of independent parameters from six to two.

For sufficiently small values of ϵ, flow properties may be expected to vary slowly with changes in the stream-wise coordinate. To incorporate this slow variation in an approximate solution we introduce the rescaled coordinate

$$\xi = \epsilon x. \tag{13}$$

In terms of the new independent variables (ξ, y), the system of differential equations becomes

$$pu = \Psi_y, \quad pv = -\epsilon\Psi_\xi, \tag{14a,b}$$

$$u_{yy} - p_\xi = \epsilon\,\text{Re}\left(\Psi_y u_\xi - \Psi_\xi u_y\right) - \frac{\epsilon}{3}v_{y\xi} - \tfrac{4}{3}\epsilon^2 u_{\xi\xi}, \tag{15}$$

$$p_y = \tfrac{4}{3}\epsilon v_{yy} + \tfrac{1}{3}\epsilon^2 u_{y\xi} - \epsilon^2\,\text{Re}\left(\Psi_y v_\xi - \Psi_\xi v_y\right) + \epsilon^3 v_{\xi\xi}. \tag{16}$$

Each dependent variable may now be expanded in a power series in ϵ, e.g.

$$u = u^{(0)}(\xi, y; \text{Re}) + \epsilon u^{(1)}(\xi, y; \text{Re}) + \text{O}(\epsilon^2). \tag{17}$$

The equations satisfied by the zero-th approximation are (14a) and (14b) through (16) with right hand sides replaced by zero. Equations (14b) and (16) immediately reveal that $v^{(0)} = 0$ and $p^{(0)}$ is a function of ξ only. Equation (15) may then be integrated immediately to yield quadratic dependence of $u^{(0)}$ on y. Substituting the expression for $u^{(0)}$ into (14a), integrating, and applying the boundary condition $\Psi^{(0)}(\xi, 1) = 1$ gives a simple ordinary differential equation for $p^{(0)}(\xi)$:

$$p^{(0)} \frac{\mathrm{d}p^{(0)}}{\mathrm{d}\xi} = -3. \tag{18}$$

Integrating (18) and applying the boundary condition $p^{(0)}(0) = 1$, we obtain the zero-th order solution

$$p^{(0)} = \sqrt{1 - 6\xi}, \quad u^{(0)} = \frac{3}{2} \frac{(1 - y^2)}{\sqrt{1 - 6\xi}}, \tag{19a,b}$$

$$\Psi^{(0)} = \frac{3}{2}\left(y - \frac{y^3}{3}\right), \quad v^{(0)} = 0. \tag{19c,d}$$

This elementary solution could have been obtained very simply by assuming that the incompressible Poiseuille solution is valid locally and finding the streamwise pressure (or density) variation that conserves mass flux down the channel. This is sometimes referred to as a 'lubrication approximation'. The present formalism has been devised so as to imbed this intuitive solution in a systematic or rational approximation scheme. Note that the solution (19) already suggests the presence of choking. Equation (19a) predicts that $p^{(0)}$ vanishes and the velocity becomes unbounded when $\xi = 1/6$. Thus there is a maximum length for continuous isothermal flows with friction; in dimensional variables this may be written

$$(L/R)_{\max} = \mathrm{Re}/(6\gamma \mathrm{M}_0^2) \tag{20}$$

where M_0 is the flow-averaged Mach number at the station from which L is measured. It follows that no steady subsonic flow with initial Mach number greater than M_0 can be maintained. This must be considered only a crude estimate of the choking length, however, since it is based only on the leading term in an infinite-series development; also equation (19b) predicts unrealistically large values of velocity as the choking station is approached.

The system of equations (14) to (16) with boundary conditions of the form (10) clearly can be solved to higher order in ϵ. Before proceeding, however, a major simplification remains to be exploited. In the above formulation, the scaled streamwise coordinate ξ is measured with respect to an arbitrarily-chosen station. Obviously the computed flow properties must be independent of this choice of reference station. This invariance or self-similarity can be used to suppress the explicit dependence of the flow properties on ξ through the introduction of a new perturbation parameter.

Consider two different reference stations, denoted by subscripts 1 and 2. Let ξ_1^* be the scaled distance of the second station referred to the first. The pressure at a third station, an unscaled distance x from the first, can be written in the form

$$\left(\frac{p}{p_{w_1}}\right)^2 = f(\xi_1, \epsilon_1; y, \mathrm{Re}) \tag{21}$$

where the subscript w denotes wall or reference pressure. For the present purpose y, like Re,

may be considered to a passive parameter. Similarly, referred to station 2, the pressure may be written, in terms of the same function f, as

$$\left(\frac{p}{p_{w_2}}\right)^2 = f(\xi_2, \epsilon_2; y, \mathrm{Re}). \tag{22}$$

The reference pressures are related by

$$\left(\frac{p_{w_2}}{p_{w_1}}\right)^2 = f(\xi_1^*, \epsilon_1; 1, \mathrm{Re}). \tag{23}$$

Combining equations (21) to (23), we obtain the functional equation

$$f(\xi_1, \epsilon_1; y, \mathrm{Re}) = f(\xi_1^*, \epsilon_1; 1, \mathrm{Re}) f(\xi_2, \epsilon_2; y, \mathrm{Re}). \tag{24}$$

From (13) we have

$$x = \xi_1/\epsilon_1 = \xi_1^*/\epsilon_1 + \xi_2/\epsilon_2$$

while (12) implies that

$$\frac{\epsilon_2}{\epsilon_1} = \left(\frac{p_{w_1}}{p_{w_2}}\right)^2.$$

These two relations may be used to eliminate ξ_2 and ϵ_2 from equation (24) which, after dropping the remaining subscript, becomes

$$f(\xi, \epsilon; y, \mathrm{Re}) = f(\xi^*, \epsilon; 1, \mathrm{Re}) f\left\{\frac{\xi - \xi^*}{f(\xi^*, \epsilon; 1, \mathrm{Re})}, \frac{\epsilon}{f(\xi^*, \epsilon; 1, \mathrm{Re})}; y, \mathrm{Re}\right\}. \tag{25}$$

This last form of the functional equation is valid for all values of ξ and ξ^*. Setting $\xi = \xi^*$ and defining the local perturbation parameter

$$\hat{\epsilon} = \epsilon/p_w^2, \tag{26}$$

the functional equation can be written as

$$\frac{p}{p_w} = P(\hat{\epsilon}; y, \mathrm{Re}). \tag{27}$$

Equation (27) merely states that the transverse pressure variation does not depend explicitly on ξ provided that it is referred to the local wall value. Recognizing that the reference velocity is inversely proportional to the reference pressure while the reference streamfunction is independent of reference pressure, we can, by a similar argument write immediately

$$u = \frac{1}{p_w} U(\hat{\epsilon}; y, \mathrm{Re}), \tag{28}$$

$$v = \frac{1}{p_w} V(\hat{\epsilon}; y, \mathrm{Re}), \tag{29}$$

and

$$\psi = \Psi(\hat{\epsilon};\ y, \mathrm{Re}). \tag{30}$$

The functional form of the streamwise wall-pressure variation may also be inferred from equation (25). Differentiating with respect to ξ, we obtain

$$f_\xi(\xi, \epsilon; 1, \mathrm{Re}) = f_1\left(\frac{\xi - \xi^*}{p_w^2}, \frac{\epsilon}{p_w^2}; 1, \mathrm{Re}\right)$$

where f_1 is the partial derivative of f with respect to the first argument. Setting $\xi = \xi^*$, we obtain

$$\frac{\mathrm{d}p_w^2}{\mathrm{d}\xi} = s(\hat{\epsilon};\ \mathrm{Re}) \tag{31}$$

where s is a function to be determined as part of the solution.

The system of equations may now be rewritten in terms of the new variables introduced in (27) to (31). The transformation of derivatives is best illustrated by an example; thus

$$u_\xi = \frac{1}{p_w} U_\xi + U\left(\frac{1}{p_w}\right)_\xi = \frac{1}{p_w} U_{\hat{\epsilon}}\, \hat{\epsilon}_\xi - \frac{U}{p_w^2} p_{w_\xi} = -\frac{s}{2p_w^3}(2\hat{\epsilon}U_{\hat{\epsilon}} + U)$$

where

$$\frac{\partial \hat{\epsilon}}{\partial \xi} = -\frac{2\epsilon}{p_w^3}\frac{\partial p_w}{\partial \xi} = -\frac{\hat{\epsilon}s}{p_w^2}$$

has been used. The full system now becomes

$$tU_{yy} - \frac{P}{2} = \hat{\epsilon}\left(-P_{\hat{\epsilon}} - \frac{\mathrm{Re}}{2}U\Psi_y + V_y/6\right) + \hat{\epsilon}^2\left(-\mathrm{Re}\ \Psi_y U_{\hat{\epsilon}} + \mathrm{Re}\ U_y\Psi_{\hat{\epsilon}} + \tfrac{1}{3}V_{\hat{\epsilon}y} - sU\right)$$

$$+\hat{\epsilon}^3\left(-4sU_{\hat{\epsilon}} - \tfrac{2}{3}s'U\right) - \tfrac{4}{3}\hat{\epsilon}^4(s'U_{\hat{\epsilon}} + sU_{\hat{\epsilon}\hat{\epsilon}}), \tag{32}$$

$$tP_y = \tfrac{4}{3}\hat{\epsilon}tV_{yy} + \hat{\epsilon}^2\left(-\frac{U_y}{6} + \mathrm{Re}\ \Psi_y\frac{V}{2}\right) + \hat{\epsilon}^3\left(\frac{U_{\hat{\epsilon}}}{3}y + \mathrm{Re}\ \Psi_y V_{\hat{\epsilon}} - \mathrm{Re}\ \Psi_{\hat{\epsilon}}V_y + \tfrac{3}{4}sV\right)$$

$$+\hat{\epsilon}^4\left(3sV_{\hat{\epsilon}} + \tfrac{1}{2}s'V\right) + \hat{\epsilon}^5(s'V_{\hat{\epsilon}} + sV_{\hat{\epsilon}\hat{\epsilon}}), \tag{33}$$

$$PU = \Psi_y, \tag{34}$$

$$PV = \hat{\epsilon}^2 s\Psi_{\hat{\epsilon}}. \tag{35}$$

In the streamwise and transverse momentum equations, (32) and (33), we have introduced the additional variable

$$t = \frac{1}{s} = \frac{\mathrm{d}\xi}{\mathrm{d}p_w^2} \tag{36}$$

in order to eliminate cubic products. Henceforth the Reynolds number will be considered to be a fixed constant; thus s' is equivalent to $ds/d\hat{\epsilon}$.

Each unknown in (32) to (36) will now be expanded as a power series in $\hat{\epsilon}$:

$$s = \sum_{i=0} s_i \hat{\epsilon}^i, \quad t = \sum_{i=0} t_i \hat{\epsilon}^i, \tag{37a,b}$$

$$U = \sum_{i=0} U_i(y)\hat{\epsilon}^i, \tag{38}$$

$$V = \sum_{i=0} V_i(y)\hat{\epsilon}^i, \tag{39}$$

$$P = \sum_{i=0} P_i(y)\hat{\epsilon}^i, \tag{40}$$

$$\Psi = \sum_{i=0} \Psi_i(y)\hat{\epsilon}^i. \tag{41}$$

We have, in addition, the boundary conditions

$$P_0(1) = 1, \quad \Psi_0(1) = 1; \quad U_i(1) = 0, \quad V_i(1) = 0, \quad i = 0, 1, \ldots;$$
$$P_i(1) = 0, \quad \Psi_i(1) = 0, \quad i = 1, 2, \ldots.$$

The coefficients s_i and t_i will be constants, for given Re, while the other subscripted variables are polynomials in y. It can be shown inductively that a sufficient assumption is

$$U_i = \sum_{j=0}^{2i+1} U_{ij} y^{2j}, \quad V_i = \sum_{j=0}^{2i} V_{ij} y^{2j+1}, \quad P_i = \sum_{j=0}^{2i} P_{ij} y^{2j}, \quad \Psi_i = \sum_{j=0}^{2i+1} \Psi_{ij} y^{2j+1}.$$

Once these expansions are substituted into the governing equations and coefficients of each power of $\hat{\epsilon}$ and y are equated, the unknowns at any order may be found as sums of products of lower-order coefficients. Details of the algorithm are given in Appendix II.

For a series solution to order $\hat{\epsilon}^N$, the computer storage required is proportional to N^2 while, consistent with the number of nested summations, the computation time varies as N^4.

An alternative method of solution, not explored in the present paper, is to attack the system of equations (32)–(36) by a finite-difference procedure. At least formally, the solution may be marched, starting with $\hat{\epsilon} = 0$ and using the zero-th order solution (19) for the initial values. The stability of such a calculation is an open question, however.

3. Discussion of results

A number of the features of the computed solutions may be surmised by inspection of the leading terms in the series expansion. To second order in $\hat{\epsilon}$, the coefficients in the series for U and Ψ may be recognized as rational numbers from their decimal expansions. Thus

$$\frac{U(\hat{\epsilon}, y)}{1-y^2} = \frac{3}{2} + \hat{\epsilon}\,\mathrm{Re}\tfrac{9}{280}(-5 + 28y^2 - 7y^4) - \hat{\epsilon}^2\left[\tfrac{9}{8}(1 + 3y^2)\right.$$
$$\left. + \frac{\mathrm{Re}^2 \cdot 27}{431200}(2193 - 9163y^2 - 6853y^4 + 5159y^6 - 616y^8)\right] + \ldots, \tag{42a}$$

$$\frac{\Psi}{y} = \frac{3}{2}\left(1 - \frac{y^2}{3}\right) + \hat{\epsilon}\,\mathrm{Re}\tfrac{9}{280}(1-y^2)^2(5-y^2)$$

$$+\hat{\epsilon}^2(1-y^2)^2\left[\frac{9}{8} + \frac{\mathrm{Re}^2\cdot 9}{431200}(-6579 - 1802y^2 + 1589y^4 - 168y^6)\right] + \ldots. \tag{42b}$$

Similarly the expansions for the transverse velocity component and the pressure are, to third order

$$V = y(1-y^2)^2\hat{\epsilon}^2\left[\frac{27\cdot \mathrm{Re}}{140}(5-y^2)\right.$$

$$\left. -\hat{\epsilon}\left\{\frac{27}{2} + \frac{27\,\mathrm{Re}^2}{107800}(-12519 - 614y^2 + 1589y^4 - 168y^6)\right\}\right] + \ldots, \tag{42c}$$

$$P = 1 + \hat{\epsilon}^2\tfrac{3}{2}(1-y^2) + \frac{\hat{\epsilon}^3\,\mathrm{Re}}{280}(873 - 2133y^2 + 1575y^4 - 315y^6) + \ldots. \tag{42d}$$

Note that both V and the cross-channel pressure variation are $O(\hat{\epsilon}^2)$; that is, for given Reynolds number, they are fourth-order in the local Mach number. For low subsonic Mach numbers, these components are quite small; they may not be negligible, however, even in engineering applications, because of their relevance to the question of stability of these laminar flows. One suspects that this may be particularly true for horizontal channel flow where the implied transverse density variation will lead to asymmetric stratification. A complete analysis must, of course, include finite Froude number, i.e. gravity, effects.

The streamwise variation in wall pressure may be extracted from the function t defined in equation (36). To second order it can be written as

$$t(\hat{\epsilon}) = \frac{\mathrm{d}\xi}{\mathrm{d}p_w^2} = -\tfrac{1}{6} + \tfrac{9}{35}\hat{\epsilon}\,\mathrm{Re} - \hat{\epsilon}^2\left(2 + \frac{156\cdot \mathrm{Re}^2}{2695}\right) + \ldots. \tag{43}$$

Recognizing that $\xi = \epsilon x$ and $\hat{\epsilon} = \epsilon/p_w^2$, we have the relation

$$\mathrm{d}x = -\frac{t(\hat{\epsilon})}{\hat{\epsilon}^2}\,\mathrm{d}\hat{\epsilon}.$$

Equation (43) may now be integrated term by term subject to the initial condition $p_w = 1$ or $\epsilon = \hat{\epsilon}$ at the reference station $x = 0$. The second-order result is

$$\epsilon x = \frac{\gamma \mathrm{M}_0^2}{\mathrm{Re}}\frac{\tilde{x}}{R} = \tfrac{1}{6}(1-p_w^2) + \tfrac{9}{35}\gamma\mathrm{M}_0^2\log p_w^2$$

$$+(\gamma\mathrm{M}_0^2)^2\left(\frac{156}{2695} + \frac{2}{\mathrm{Re}^2}\right)\left(\frac{1-p_w^2}{p_w^2}\right) + \mathrm{O}(\gamma\mathrm{M}_0^2)^3. \tag{44}$$

Here we have used the definition $\epsilon = \mathrm{M}_0^2/\mathrm{Re}$ where M_0 is the reference or 'entry' Mach number at $x = 0$. Notice that the M_0^2 term or the right side of (44) is negative, leading to the possibility of a maximum length for continuous isothermal flow, i.e. the choking phenomenon.

The algorithm described in the preceding section has been programmed in FORTRAN and run to order ϵ^{40} for a range of Reynolds numbers from 0 to 1000. The fortieth-order solution

required several seconds of central processor time and about 20000 words of storage. By running in both single and double precision, it is possible to assess the importance of round-off error. Typically round-off error resulted in the loss of one significant figure for every three orders in ϵ. It should be noted that round-off is much more important in high-order series methods than in standard finite-difference or finite-element methods since the Padé table extracts information from the least significant portion of each coefficient.

It is often possible to use the results of a high-order series solution to infer information about the singularity structure of an unknown function. For example, if the ratio of successive Taylor series coefficients, a_n/a_{n-1} say, tends to approximate linear variation with $1/n$, one may, by comparison with the coefficient behavior of the binomial expansion, estimate the location of the singularity that limits convergence and the 'critical' behavior near that point. On the other hand, if the unknown function possesses a number of singularities, with none clearly closest or strongest, the series coefficients will be erratic. However, it may still be possible to roughly predict the radius of curvature or, at a minimum, to determine whether the series is convergent at all for sufficiently small values of the parameter.

Table 1 shows coefficients t_n in the series (43) through 20th order for several values of Re. Their behavior reflects the fact that the coefficient of ϵ^n is a polynomial of order Re^n that contains only even or odd order terms as n is even or odd. No definite structure is apparent in any of the series except for the general rate of growth of the coefficients with increasing n. The pattern of signs is irregular in general, a pattern which continues up at least 40th order in ϵ. For small values of Re, the magnitude of the coefficient growth suggests a radius of convergence in the complex ϵ-plane of order 10^{-1}. From the series for $\mathrm{Re} = 100$ and 1000, it is apparent that the coefficients scale like Re^n; thus a more appropriate parameter for large Reynolds number is $\epsilon\mathrm{Re} = \gamma\mathrm{M}^2$. The rate of growth and the pronounced irregularities in these series suggest the presence of several singularities at a distance of about 1.0 in the γM^2-plane. If one of these singularities lies on the positive real axis, the convergence limit for the series solution could be due to a physical singularity corresponding to choking due to local velocities near the sound speed.

Table 1. Coefficients in the series $\sum t_n \epsilon^n$.

n	Re = 0	Re = 1	Re = 100	Re = 1000
0	−0.1667	−0.1667	−0.1667	−0.1667
1	0	0.2571	2.5714E01	2.5714E02
2	−2.000	−2.0579	−5.8085E02	−5.7887E04
3	0	−5.3298	−7.8894E04	−7.8375E07
4	7.1271E01	6.5560E01	−2.307E06	−2.2645E10
5	0	3.8847E02	9.0429E08	9.0147E13
6	−3.9692E03	−3.1106E03	7.3379E10	7.2620E16
7	0	−2.8320E04	−1.5765E13	−1.5689E20
8	2.4695E05	1.4870E05	−1.5310E15	−1.4974E23
9	0	2.433E06	3.2813E17	3.2922E26
10	−2.4137E07	−6.0298E06	2.1500E19	2.1327E29
11	0	−3.2371E08	−6.3514E21	−6.2733E32
12	2.6543E09	−3.4133E08	−2.1140E23	−1.9954E35
13	0	2.2226E10	8.8076E25	8.7428E38
14	−1.3289E11	6.5945E10	6.4750E27	6.3484E41
15	0	−4.8655E12	−2.1021E30	−2.0781E45
16	1.3671E14	−7.4087E13	1.0342E31	1.39807E47
17	0	1.6324E15	1.4233E33	8.8912E49
18	3.2267E16	−1.0497E16	1.1967E37	1.1895E55
19	0	1.4523E18	−4.5032E39	−4.4944E58
20	4.3502E18	−1.224E18	1.570E42	1.5729E62

Even when the singularity structure of a power series is not known, it can often be summed to high accuracy by the use of Padé approximants. A diagonal Padé approximant is a ratio of two polynomials, each of order N, whose coefficients are selected so that the rational fraction, when expanded for small argument, agrees with the power series from which it is formed to (at least) order $2N$. Symbolically we write, for a function $f(x)$,

$$f(x) \sim \sum_{n=0}^{2N} f_n x^n + \mathrm{O}(x^{2N+1}) \sim \frac{a_0 + a_1 x + \ldots + a_N x^N}{1 + b_1 x + \ldots + b_N x^N} + \mathrm{O}(x^{2N+1})$$

$$\triangleq [N/N]f + \mathrm{O}(x^{2N+1}).$$

Provided that the closest singularity of f does not lie on the positive real x-axis, the sequence of approximations can be expected to converge much faster, for $x > 0$, than the series from which they are formed and will, in fact, converge for values of x for which the original series diverges. Details of the theory of Padé approximants and examples of their successful application to problems in fluid mechanics and solid-state physics may be found in the book edited by Cabannes [3]. In the results presented below, the series have been summed by diagonal Padé approximants that have converged to at least graphical accuracy.

In Figs. 1 and 2 we show the variation in wall pressure with distance for large and small values of Reynolds number. This behavior is calculated from a high-order version of the expansion (44) that has been summed with the aid of Padé approximants. Specifically we have

$$\frac{\tilde{x}}{R} = \frac{\mathrm{Re}}{\gamma \mathrm{M}_0^2} \left\{ \tfrac{1}{6}(1 - p_w^2) + \tfrac{9}{35}\gamma \mathrm{M}_0^2 \log p_w^2 + \frac{(\gamma \mathrm{M}_0^2)^2}{\mathrm{Re}^2} \left([N/N]F(\epsilon) - \frac{[N/N]F(\epsilon/p_w^2)}{p_w^2} \right) \right\} \tag{45}$$

where

$$F(\epsilon) = t_2 + \frac{t_3}{2}\epsilon + \ldots + \frac{t_{j+2}}{j+1}\epsilon^j + \ldots$$

and $[N/N]F(\epsilon)$ is a diagonal Padé approximant computed from this series. Figure 1 gives the

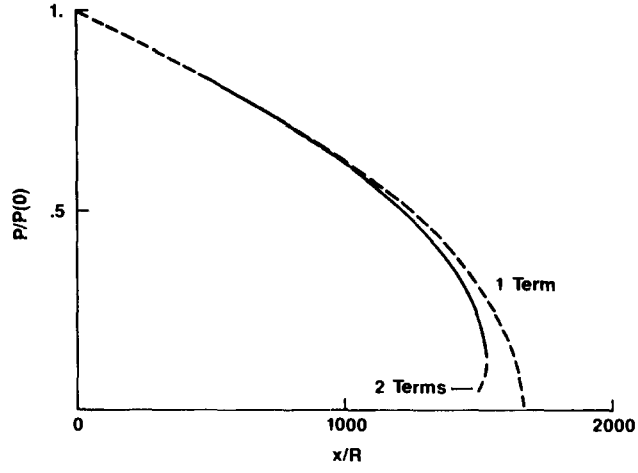

Fig. 1. Wall pressure variation with distance; $\mathrm{Re} = 100$, $\gamma \mathrm{M}_0^2 = 0.01$. ——— Padé [5/5], [6/6].

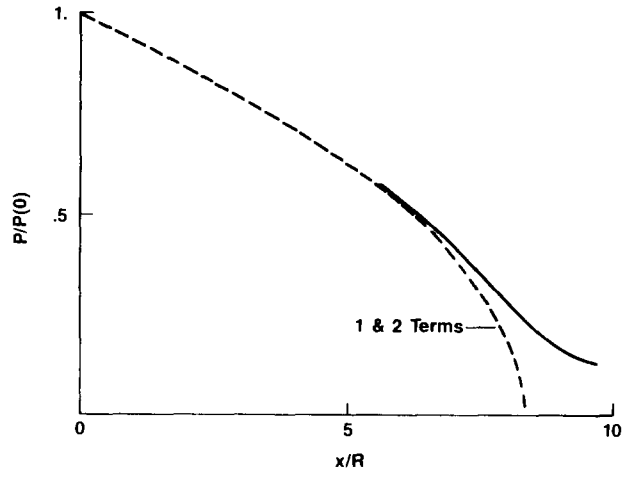

Fig. 2. Wall pressure variation with distance; Re = 0.01, $\gamma M_0^2 = 0.0002$. ——— Padé [5/5], [6/6].

results for a channel half-width Reynolds number of 100 and an initial value of Mach number parameter $\gamma M_0^2 = 0.01$. The one- and two-term approximations are indicated by dashed lines. The solid curve is, in fact, two curves drawn using expression (45) with $N = 5$ and 6 respectively. Within graphical accuracy, the Padé approximants agree with one another and also with the two-term approximation. This latter result predicts choking, i.e. a maximum length for continuous isothermal flow, when $t = d\xi/dp_w^2 = 0$ or, using two terms in equations (43), when

$$\gamma M_l^2 = \tfrac{35}{54}. \tag{46}$$

Here M_l is the station-averaged local Mach number. Since the centerline Mach number is larger than M_l by a factor of about 1.5, the centerline condition at this critical station is approximately sonic. The critical station is located 1530 half-widths downstream of the reference station and the critical wall pressure is about 1/8 of the reference value. One may infer that a further reduction in the downstream pressure will not result in a corresponding increase in the mass flow rate.

The situation is rather different at low values of Re. Figure 2 shows the pressure variation for Re = 0.01. The one- and two-term approximations are virtually coincident while the Padé-summed results deviate markedly and exhibit a pronounced inflection point. Thus the maximum length for continuous isothermal flow is longer than would be predicted by the low-order expressions. The largest value of x/R shown in Fig. 2 corresponds to a local value of $\gamma M^2 \cong 0.11$. For small Reynolds number, flows at near-sonic conditions cannot be predicted with confidence; the loss of accuracy may well be due to the development of a complicated flow structure, rather than incipient choking.

Transverse pressure profiles are shown in Figs. 3 and 4 for $\sqrt{\gamma}\,M = 0.316$ and 0.775 respectively. The Reynolds number for both cases is 10. Therefore these profiles show that transverse pressure gradients develop, within a channel, as the longitudinal flow accelerates to compensate for the reduced mass flow as the pressure, or density, is reduced. The dashed line is the second-order result

$$p/p_w \cong 1 + \epsilon^2(3/2)(1 - y^2), \tag{47}$$

which, when compared with the converged Padé results is seen to be a reasonable approxima-

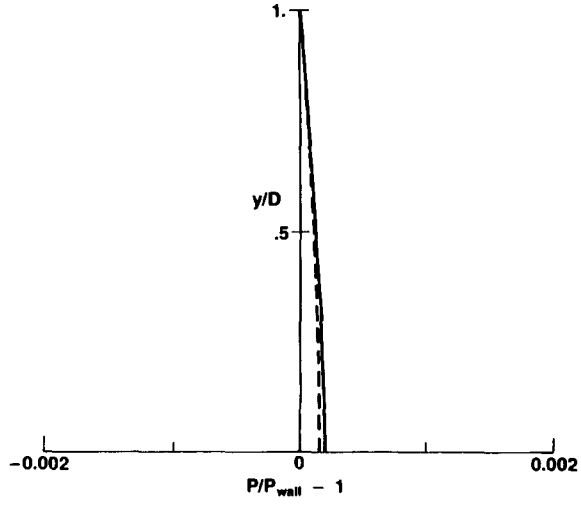

Fig. 3. Transverse pressure profile, Re = 10, $\sqrt{\gamma}\,M = 0.316$. - - - - - - second-order theory, ——— Padé approximants.

tion at the lower Mach number. In Fig. 4, on the other hand, equation (47) grossly underpredicts the pressure difference between the centerline and the wall, which in this case is about 4 per cent. In all cases it appears that the pressure in the middle of the channel exceeds the value on the wall at a given station. Note also that the minimum pressure, in Fig. 4, occurs not at the wall but at $y/D \cong 0.9$.

A typical horizontal velocity profile is shown in Fig. 5. We see that the effect of finite Mach number is to flatten the profile relative to the incompressible Poisseuille parabolae, the effect becoming more pronounced as the Mach number is increased. For comparison, the vertical component of velocity, between the centerline and the upper wall are shown in Fig. 6 for a large and small value of Reynolds number. The vertical velocity is always small corresponding to a maximum streamline inclination of about 0.5 degree in each case. For large Re the flow is inclined towards the channel wall, while for Re = 0.01 the flow is generally tilted towards the channel centerline.

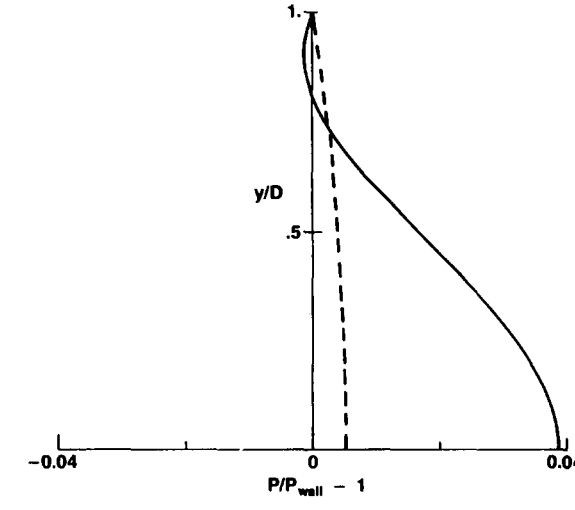

Fig. 4. Similar to Fig. 3, except $\sqrt{\gamma}\,M = 0.775$.

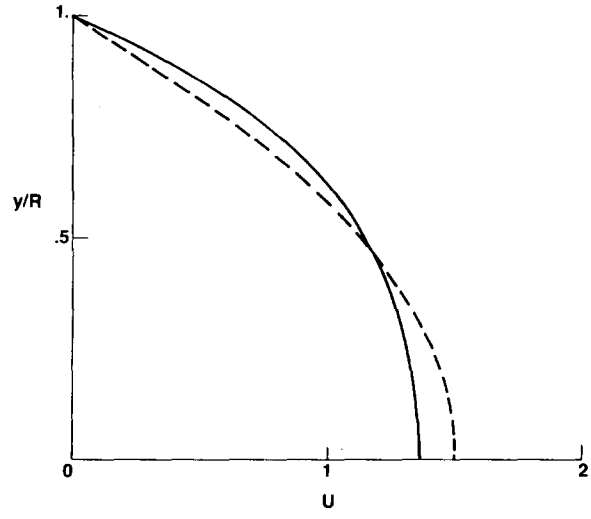

Fig. 5. Horizontal velocity profile, Re = 100, $\sqrt{\gamma}\,M = 0.775$, - - - - - - Poiseuille flow, ——— [6/6] Padé approximant.

A quantity of significant engineering interest is the shear stress τ_w at the channel wall. It is usual practice in order to assess the effects of compressibility, to refer τ_w to the local dynamic head $\tilde{q}$ to form a dimensionless coefficient usually called the skin friction coefficient or the friction factor in hydraulics. In terms of local reference quantities, we have

$$\tilde{q} = \tfrac{1}{2}\rho_{\text{ref}} u_{\text{ref}}^2 = \frac{\dot{m}^2}{2\rho_w R^2}$$

Since $\tau_w = \mu \partial \tilde{u}/\partial \tilde{y}\,|_{\tilde{y}=R}$ one finds, for the friction factor f_1, in dimensionless units,

$$f_1 = -\frac{2}{\text{Re}} \left.\frac{dU}{dy}\right|_{y=1}. \tag{48}$$

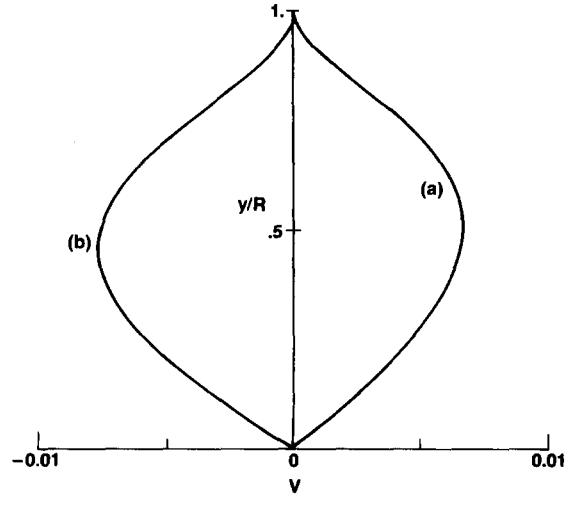

Fig. 6. Two vertical velocity profiles. (a) Re = 100, $\sqrt{\gamma}\,M = 0.775$, ($\epsilon = 0.006$); (b) Re = 0.01, $\sqrt{\gamma}\,M = 0.045$, ($\epsilon = 0.2$).

Expressing the right side of (48) as a series in $\hat{\epsilon}$, we have, through second order,

$$f_1 = f_{\text{inc}}\left[1 + \hat{\epsilon}\,\text{Re}\tfrac{12}{35} + \hat{\epsilon}^2\left(-3 + \tfrac{1251}{3080}\,\text{Re}^2\right) + O(\hat{\epsilon}^3)\right] \tag{49}$$

where

$$f_{\text{inc}} = \frac{6}{\text{Re}} \tag{50}$$

is the friction factor for incompressible flow. (Note that the numerical constant in equation (50) becomes 12 if the channel width or the hydraulic radius is used as reference length or 24 if the unit of length is the hydraulic diameter.) Thus the quantity in square brackets in (49) can be interpreted as a correction factor due to finite Mach number. It is interesting to note that in turbulent pipe flows it is apparently standard practice to ignore compressibility for virtually all subsonic Mach numbers (See Shapiro [10, p. 184]).

The friction factor discussed above turns out not to be the usual one. Using one-dimensional gasdynamic and a simple momentum balance, Shapiro [10] obtains, in effect,

$$f_2 = -\frac{2R}{p}\frac{\mathrm{d}p}{\mathrm{d}\tilde{x}}\frac{\left(1-\gamma \text{M}_l^2\right)}{\gamma \text{M}_l^2}. \tag{51}$$

The friction factor f_2 is nominally defined as $\tau_w/\tilde{q}$ just as is f_1. However, the simple theory is apparently defective; this anomaly is discussed in Appendix I. It may be useful to regard f_2 are merely a special nondimensional representation of the pressure gradient. By calculating f_2 according to (51), the defective one-dimensional theory can be made to yield correct results for the pressure drop in laminar channel flow. In terms of the dependent variable $t(\hat{\epsilon};\ \text{Re})$ defined in equation (36), f_2 may be written as

$$f_2 = -\frac{\left(1-\gamma \text{M}_l^2\right)}{\text{Re}\,t} \tag{52}$$

which may be expanded as

$$f_2 = f_{\text{inc}}\left[1 + \tfrac{19}{35}\hat{\epsilon}\,\text{Re} - \hat{\epsilon}^2\left(12 - \tfrac{46242}{94325}\,\text{Re}^2\right) + O(\hat{\epsilon}^3)\right]. \tag{53}$$

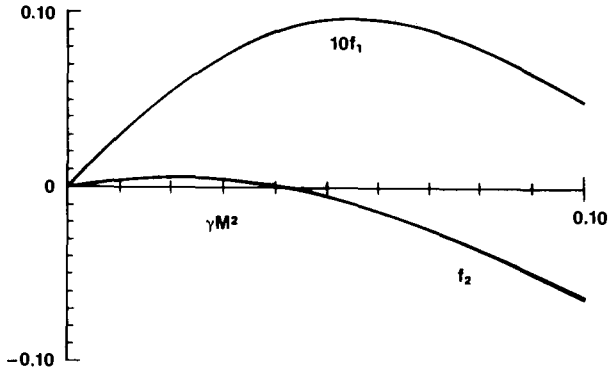

Fig. 7. Fractional change in friction factors due to finite Mach number using Padé summation. The vertical axis is $f/f_{\text{incompressible}} - 1$. f_1 and f_2 are defined in equations (48) and (51) respectively; Re = 1.

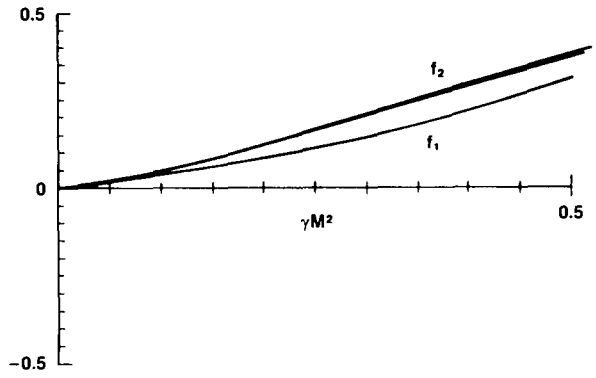

Fig. 8. Similar to Fig. 7, except Re = 100.

Comparing this expansion with (49), it may be seen that the leading-order compressibility terms differ by a factor of 19/12.

In order to assess the effects of compressibility on friction factor for the isothermal, laminar flow considered here, high-order versions of equations (49) and (53) have been recast as sequences of Padé fractions for several values of Re. In Figs. 7 and 8 we show Padé-summed results for f_1 and f_2 as functions of γM^2. Each curve shown is, in fact, four distinct curves, the [3/3] through [6/6] Padé approximants plotted upon one another so as to illustrate the degree of convergence of each sequence. A slight broadening of each 'curve' can be observed at the larger values of γM^2. Results for the smaller Re cases seems to validate the engineering hypothesis that compressibility effects are minor, at least for the range of Mach numbers shown in Fig. 7. The situation is quite different for Re = 100 (fig. 8). Here neglect of compressibility results in a significant underprediction of effective skin friction. For $\gamma M^2 = 0.5$, for example, f_1 and f_2 exceed the incompressible value by about 30 and 40 per cent respectively.

Appendix I

On the one-dimensional theory of viscous compressible flow

Most books on gasdynamics or hydraulics that consider compressible flow with friction (e.g. Shapiro [10, p. 162]) find an expression for the skin friction using a simple one-dimensional theory. It is the purpose of this appendix to explain why the leading-order effect of compressibility on the skin friction is predicted incorrectly, especially in the laminar flow regime.

In the one-dimensional theory one assumes that pressure $\bar{p}$, density $\bar{\rho}$, and velocity $\bar{u}$ are functions of x only. A momentum balance over an elemental area of length $\mathrm{d}x$ and constant width $2R$ immediately yields

$$-R\,\mathrm{d}\bar{p} - \tau_w\,\mathrm{d}x = R\,\mathrm{d}(\bar{\rho}\bar{u}^2) = R\bar{\rho}\bar{u}\,\mathrm{d}\bar{u}. \tag{A.1}$$

Here we have used the continuity equation $\bar{\rho}\bar{u} =$ constant. Equation (A.1) may now be compared with the integrated form of the two-dimensional x-momentum equation. The latter may be written as

$$\rho(uu_x + vu_y) = -p_x + \mu u_{yy} + \tfrac{4}{3}\mu u_{xx} + \tfrac{1}{3}\mu v_{yx}. \tag{A.2}$$

Integrating each term in (A.2) over $(0, R)$ and denoting averages by an overbar, we obtain

$$\int_0^R p_x\,\mathrm{d}y = R\frac{\mathrm{d}\bar{p}}{\mathrm{d}x}, \tag{A.3}$$

$$\int_0^R \mu u_{yy}\,\mathrm{d}y = \mu \frac{\partial u}{\partial y}\bigg|_{y=R} = -\tau_w, \tag{A.4}$$

$$\int_0^R v_{xy}\,\mathrm{d}y = v_x\big|_{y=R} - v_x\big|_{y=0} = 0. \tag{A.5}$$

The integral

$$\int_0^R \mu u_{xx}\,\mathrm{d}y = \mu R \bar{u}_{xx}$$

is, in fact, not zero but a positive quantity. It represents the contribution of dilation to the normal stress and is incorrectly omitted from (A.1). It is, however, $O(\hat{\epsilon}^2)$ and thus does not account for the leading-order discrepancy. The integral of the convective term, on the other hand, becomes

$$\int_0^R \rho(uu_x + vu_y)\,\mathrm{d}y = \int_0^R \rho u u_x\,\mathrm{d}x - \int_0^R u(\rho v)_y\,\mathrm{d}x = \frac{\mathrm{d}}{\mathrm{d}x}\int_0^R \rho u^2\,\mathrm{d}y$$

$$= \frac{\mathrm{d}}{\mathrm{d}x}\overline{\rho u^2} = \frac{\mathrm{d}}{\mathrm{d}x}\bar{\rho}\overline{u^2} + O(\hat{\epsilon}^2). \tag{A.6}$$

Here we have integrated by parts and used the two-dimensional continuity equation. Also, in the last line, we use the fact that the transverse density variation is $O(\hat{\epsilon}^2)$. Combining the above results, and using a form equivalent to (A.1), we write

$$-R\,\mathrm{d}\bar{p} - \tau_w\,\mathrm{d}x = R\,\mathrm{d}\left(\bar{p}\overline{u^2}\right) + O(\hat{\epsilon}^2) = R\bar{\rho}\bar{u}\,\mathrm{d}\left(\frac{\overline{u^2}}{\bar{u}}\right) + O(\hat{\epsilon}^2). \tag{A.7}$$

The error in the friction factor at $O(\hat{\epsilon})$ can now be seen to arise from replacing $\overline{u^2}$ by $\bar{u}^2$. In a turbulent flow, the mean velocity profile is rather flat and these quantities may almost be equal. In the laminar regime, however, this replacement causes a significant error.

Appendix II

The recurrence relations for generating the series coefficients

The partial differential equations (32) through (35) in Section 2 become, after insertion of the double-series expansions,

$$-\tfrac{1}{3}(j+1)(2j+1)U_{k,j+1} = -\left(k-\tfrac{1}{2}\right)P_{kj} + \left(\frac{2k-1}{6}\right)(2j+1)V_{k-1,j} - 2(j+1)(2j+1)\sum_{i=1}^{k-1} U_{i,j+1}t_{k-i}$$

$$+ \mathrm{Re}\sum_{i=0}^{k-1}\sum_{l=0}^{j} U_{il}\Psi_{k-1-i,j-l}\left(2kl - l - 2ij - \tfrac{1}{2}i - j\right)$$

$$+ \tfrac{1}{3}\sum_{i=0}^{k-2} U_{ij}s_{k-2-i}(1+2i-2k-4ik),$$

$$P_{kj} = (2k-3)U_{k-2,j} - 8(2j+1)\sum_{i=0}^{k-1} t_{k-1-i}V_{ij} + 6\sum_{i=1}^{k-1} t_{k-i}P_{ij}$$

$$-3\frac{\mathrm{Re}}{j}\sum_{i=0}^{k-2}\sum_{l=0}^{j-1} V_{il}\Psi_{k-2-i,j-l-1}\left[2j\left(i+\tfrac{1}{2}\right) - (2l+1)\left(k-\tfrac{3}{2}\right)\right]$$

$$-\frac{3}{j}\sum_{i=0}^{k-3} V_{i,j-1}s_{k-3-i}\left(-\tfrac{3}{4} - \tfrac{3}{2}i + \frac{k}{2} + ik\right), \tag{A.9}$$

$$(2j+1)\Psi_{kj} = \sum_{i=0}^{k-1} \sum_{l=0}^{j} U_{il} P_{k-i,j-l} + U_{kj}, \tag{A.10}$$

$$V_{kj} = \sum_{i=1}^{k-1} \left(i\Psi_{ij} s_{k-1-i} - \sum_{l=0}^{j} V_{il} P_{k-i,j-l} \right). \tag{A.11}$$

All sums are taken to be identically zero when the lower limit exceeds the upper. Similarly, coefficients with either subscript negative are also identically zero. Subject to the expanded form of the boundary conditions given in Section 2, a simultaneous solution of these algebraic equations may be found for each pair of integers (k, j).

References

1. Abramowitz, M.: On backflow of a viscous fluid in a diverging channel, *J. Math. Phys.* 28 (1949) 1–21.
2. Blasius, H.: Laminare Strömung in Kanälen wechselnder Breite, *J. Math. Phys.* 58 (1910) 225–233.
3. Cabannes, H. (ed.): *Padé Approximants Method and Its Application to Mechanics*, Springer-Verlag, Berlin, New York (1976).
4. Fox, J.A.: *Hydraulic Analysis of Unsteady Flow in Pipe Networks*, Wiley, New York (1977).
5. Gross, W.A.: *Gas Film Lubrication*, Wiley, New York (1968).
6. Lagerstrom, P.A., Laminar flow theory, in: *Theory of Laminar Flows*, F.K. Moore (ed.), Princeton Univ. Press (1964) 20–285.
7. Lucas, R.D.: A perturbation solution for viscous flow in channels, Ph.D. Dissertation, Stanford University (1972).
8. Pai, S.-I.: *Viscous Flow Theory, I - Laminar Flow*, Van Nostrand, Princeton, N.J. (1956).
9. Schlichting, H.: *Boundary-Layer Theory*, McGraw-Hill, New York (1968).
10. Shapiro, A.H.: *The Dynamics and Thermodynamics of Compressible Fluid Flow, Vol. 1*, Ronald Press, New York (1953).
11. Van Dyke, M.D.: Slow variations in continuum mechanics, *Advances in Applied Mechanics* 26 (1986) (in press).